Effect of homogenization treatments on recrystallization behavior of 7150 aluminum alloy during post-rolling annealing

Zhanying Guo [a,b], Gang Zhao [a], X.-Grant Chen [b,*]

[a] Key Laboratory for Anisotropy and Texture of Materials,

Northeastern University, Shenyang, China, 110819

[b] Department of Applied Science, University of Québec at Chicoutimi,

Saguenay (QC), Canada G7H 2B1

Abstract

The effect of two-step homogenization treatment on the recrystallization behavior in 7150 Al alloy during isochronal annealing after cold-rolling in the temperature range of 200 ºC to 500 ºC has been investigated. Two-step homogenization with the first step treated at 250 ºC followed by the second step at 470 ˚C were applied. It is found that, much higher number density and smaller size of Al_3Zr dispersoids were obtained after two-step homogenization, which strongly pin subgrain boundaries and inhibiting recrystallization significantly. Compared with conventional one-step homogenized samples with a partial recrystallized microstructure which is dominant of elongated coarse grains for annealing beyond 350 ºC, the deformed structure was present in the two-step homogenized samples for all annealing conditions. The effect of two-step homogenization on the recrystallization behavior was quantitatively analyzed using the data derive from EBSD technique. Two-step homogenization results in low recrystallized fraction and small recrystallized grain size under all annealing conditions. In addition, lower average misorientation and smaller cell size were obtained after two-step homogenization applied.

Keywords: 7150 Al alloy, Two-step homogenization, Recrystallization, Al_3Zr dispersoids, Zener drag.

* Corresponding author:

X.-Grant Chen

Department of Applied Science, University of Québec at Chicoutimi

Saguenay (QC), Canada G7H 2B1

Tel.: 1-418-545 5011 ext. 2603; Fax: 1-418-545 5012

E-mail: xgrant_chen@uqac.ca

1. Introduction

High strength Al-Zn-Mg-Cu (7xxx series) rolling plates are widely used in aeronautical and astronautic industries because of their high strength to density ratio and excellent mechanical properties [1-4]. To obtain essential properties of high strength and fracture toughness, these alloys are subject to complex fabrication routes which involve thermomechanical deformation and thermal treatments. Rolling (hot and cold) and annealing are two critical processes for the conventional fabrication routes of these high strength alloys. However, the mechanical properties of final products are often deteriorated by recrystallization that occurs mainly during post-rolling annealing. Moreover, the fracture toughness of 7xxx Al alloys decreases with the increasing of recrystallization degree that occurs during thermomechanical deformation and subsequent annealing [4]. Therefore, the recrystallization is highly undesired and the recrystallized fraction should be greatly minimized. Recrystallization that occurred during annealing can be inhibited by the presence of second particles which exert retarding force (Zener-drag) on moving grain and subgrain boundaries [5-7]. As recrystallization inhibitor, the effectiveness of the second particles strongly depends on their size, number density and distribution [6, 7].

The addition of small quantities of Zr to 7xxx alloys can enhance the recrystallization resistance by forming fine and thermal stable Al_3Zr dispersoids during homogenization treatment of the cast billets [7]. To date, the effect of both Zr content and homogenization condition on the precipitation behavior of Al_3Zr dispersoids and the recrystallization resistance in 7xxx alloys have been investigated by several works [8-11]. However, due to the peritectic solidification of Al-Zr system and a low diffusivity of Zr in Al [12-15], it is difficult to remove the concentration gradients of Zr in solid solution during conventional one-step homogenization treatment. After conventional one-step homogenization, Al_3Zr dispersoids were heterogeneously distributed within aluminum matrix [13-15] and the precipitate free zone of Al_3Zr dispersoids would be formed in interdendritic regions which both were prone to recrystallization [8, 16]. Therefore it is possible to increase the effectiveness of the Al_3Zr dispersoids as recrystallization inhibitor by optimising homogenization practice and condition. To improve the recrystallization resistance, there is limited number of research works exploring stepwise homogenization to optimize the homogenization condition of Zr containing aluminium alloys [16-20]. It was suggested that a denser and more homogeneous distribution of Al_3Zr dispersoids could be formed and a smaller recrystallized fraction were thus obtained using stepwise homogenization. In our

recent work [21], the effect of different two-step homogenization treatments on the precipitation of Al_3Zr dispersoids (size and distribution) was studied. It was fond that the two-step homogenization produced a finer particle size and higher number density of Al_3Zr dispersoids and minimized the precipitate free zones, which resulted in a remarkable increase of the recrystallization resistance during post-deformation annealing. However, there is still a lack of quantitative study of the effect of stepwise homogenization on the evolution of the recrystallization process during post-rolling annealing in 7150 aluminum alloy.

In the present study, DC cast 7150 alloy containing 0.13% Zr were subject to different homogenization treatments, followed by multi-pass hot and cold rolling and subsequent annealing. The investigation was initiated to compare the Al_3Zr dispersoids distribution caused by one-step and two-step homogenization practices. The effect of two-step homogenization on recrystallization behavior during isochronal annealing after cold rolling over a wide range of temperatures was quantitatively analyzed using EBSD technique.

2. Experimental

The material used in this study was a 7150 aluminum alloy with 0.13% Zr and the chemical composition is presented in Table 1 (all compositions are in wt% unless otherwise indicated). The initial material was a direct chill (DC) cast billet with a diameter of Ø100 mm. The cast billet was homogenized in an air circulation furnace, followed by water quenching. The homogenization processes included both conventional one-step homogenization where samples were held at 470 ºC for 24 h, and new two-step homogenization where sample was heat-treated at the temperature of 250 ˚C for 24 h in the first step and followed at 470 ºC for 24 h in the second step. Rectangle pieces of 40 mm x 40 mm sectioned from the as-homogenized billet were hot-rolled to 7 mm plates by 8 passes at 400 ºC (a reduction of 82%). These plates were inter-annealed in an air furnace at 400 ºC for 2 h and then cooled in the furnace to room temperature. The annealed plates were subsequently cold-rolled at room temperature to final 2 mm sheets after 6 passes (a reduction of 74%). The cold-rolled sheets were subsequently and isochronally annealed at the temperature range of 200 to 500 ºC for 1 h, followed by water quench.

Vickers microhardness measurements were performed on the cross-section of isochronally annealed sheets. A load of 500 g was applied for a dwell time 20 s on polished surface. The data were reported using an average value of at least 15 measurements. The examinations of intermetallic particles were observed using the backscattered electron (BSE) detector in a scanning electron microscopy (JEOL JSM-6480LV). Electron backscattered

diffraction (EBSD) measurements were performed in the scanning electron microscopy using HKL Channel 5 software. For the EBSD data analysis, to define the subgrain boundary and size developed during deformation and annealing, a misorientation threshold value of 2º was selected [22]. The boundaries with misorientations between 2º and 15º were defined as low angle grain boundaries and those of misorientation >15º as high angle grain boundaries. Low angle grain boundaries are depicted as white lines and high angle grain boundaries as black lines in all images. The grains whose internal misorientation is lower than 1° and with grain size larger than 3 times of the scanning step size are defined as recrystallized. All the remaining grains are classified as unrecrystallized. For all the micrographs presented in this study, the horizontal direction and the vertical direction correspond to the rolling direction (RD) and normal direction (ND), respectively.

A transmission electron microscope (TEM, JEOL JEM-2100) was used to study the precipitation of Al_3Zr dispersoids during homogenization. TEM samples were mechanically ground to ~ 40 μm thickness, followed by twin-jet electropolishing at 15 V DC in a 30% nitric acid and 70% methanol solution cooled to ~ 25 ºC. The TEM examination was performed with the specimen oriented along low index [011] zone axis of Al matrix, utilizing two-beam diffraction conditions. To determine the dispersoids volume fraction and number density, the thickness of the TEM foils was measured using an Electro Energy Loss Spectroscopy (EELS) attached in the TEM. The average radius, number density and volume fraction of the dispersoids were quantified by image analysis of digitized TEM images.

3. Results and discussion

3.1 Microstructure of as-cast and homogenized samples

In the as-cast condition, the 7150 alloy sample was characterized by many dendrite α-Al cells surrounded by a network of intermetallic compounds in interdendritic regions (Fig. 1a). Under a high magnification of backscattered SEM image (Fig. 1b), it revealed that this alloy contained three main intermetallic phases distributed in interdendrite boundaries. Base on previous works of 7xxx alloys [23, 24] and SEM-EDS analysis, the brightest droplets were identified to be θ(Al_2Cu) and the bright irregular shape phase was η($MgZn_2$). The grey coarse phase was determined to be S(Al_2CuMg) intermetallic phase. Compared to η($MgZn_2$) and S(Al_2CuMg) phases, the θ(Al_2Cu) phase is present in rather small fraction. In the etched optical image, the as-cast sample was composed of coarse equiaxed grain structure with an average grain size of ~120 μm (Fig. not showing).

After one-step and two-step homogenization treatments (Fig. 2), the low melting point intermetallic phases η($MgZn_2$) and θ(Al_2Cu) were completely dissolved into the aluminum matrix, whereas the coarse intermetallic phases of S(Al_2CuMg) were fragmented and only partially dissolved, which is consist with previous works [23, 24]. There was a considerable amount of undissolved S(Al_2CuMg) retained in the original interdendritic boundaries. Image analysis results suggested a similar fraction of this phases remained in the microstructure for both one-step and two-step homogenized samples.

During homogenization, fine Al_3Zr dispersoids precipitate in aluminum matrix in Zr contained 7xxx alloys [21]. Fig. 3 shows typical TEM dark field images of the Al_3Zr dispersoids after both one-step and two-step homogenization treatments. Compared with the one-step homogenized sample, a significantly smaller size of Al_3Zr dispersoids with a considerably higher number density was obtained in the two-step homogenized sample. Moreover, in the two-step homogenized sample, the interparticle space between the dispersoids was much smaller and the distribution of Al_3Zr became more homogenous. It indicated that the first step treatment at the lower temperature (250 ˚C) in the two-step homogenization produced more Al_3Zr nuclei relative to the one-step homogenization, due to high Zr supersaturation at the low temperature. However, those small nuclei/dispersoids can only slowly grow at the low temperature, attributed to the low diffusion rate of Zr at the low temperature. The subsequent second step treatment at high temperature (470 ˚C) provides a normal condition for their growth. Overall, much denser and finer dispersoids were obtained when the two-step homogenization was applied. Table 2 shows the radius, number density

and volume fraction of Al_3Zr dispersoids after one-step and two-step homogenization treatments. It can be seen that the average sizes of Al_3Zr dispersoids are ~18.9 nm and ~ 7.8 nm for one-step and two-step homogenized samples, respectively. The difference in volume fractions of Al_3Zr dispersoids is almost negligible between one-step and two-step homogenized samples. Therefore, a much higher number density of Al_3Zr dispersoids in the two-step homogenized sample can be produced.

3.2 Microstructure evolution after hot rolling and subsequent annealing

Fig. 4 shows typical EBSD images of the grain structure for both one-step and two-step homogenized samples after hot rolling and subsequent annealing. As seen in Fig. 4a, b, after hot rolling the original equiaxed grains were severely deformed into elongated grain structure which was paralleled to the rolling direction. The high-angle grain boundaries ($\theta > 15^o$) were mainly distributed between the elongated bands and aligned with the rolling direction. Furthermore, a high density of low-angle boundaries ($2^o \leq \theta \leq 15^o$) can be observed within elongated grains, indicating a large number of subgrains were formed and a remarkable dynamically recovery occurred during hot rolling. For the one-step homogenized sample (Fig. 4a), in addition to the development of recovery structure, dynamic recrystallization might also occurr during hot rolling. A number of fine equiaxed grains with high-angle boundaries that contained substructures were observed along the serrated grain boundaries, although the recrystallization fraction is limited to few percentages (3-5%). However, no evidence was found to suggest any recrystallization taken place during hot rolling and only dynamically recovered structure was observed in the two-step homogenized sample (Fig. 4b). Subgrains with neatly arranged boundaries were uniformly formed within elongated grains. After subsequent annealing at 400 ^oC for 2h, the one-step homogenized sample (Fig. 4c) was significant recrystallized and the microstructure was characterized by a large part of slightly elongated recrystallized grains along the rolling direction, which had a recrystallized fraction of ~ 61% with an average recrystallized grain size of ~ 21 μm. With respect to the two-step homogenized sample (Fig. 4d), the majority of the microstructure was typically recovered grain structure in which the elongated bands were clearly seen after annealing. There are only few small recrystallized grains distributed heterogeneously along the bulged grain boundaries and the recrystallized fraction was ~ 8% with an average recrystallized grain size of ~ 10 μm. It is fair to conclude that the improvement of Al_3Zr size and distribution by two-step homogenization results in the inhibition of recrystallization during hot rolling and subsequent

annealing. The strong effect of the two-step homogenization on the improved recrystallization resistance is particularly showed during post-rolling isochronal annealing.

3.3 Effect of homogenization treatments on recrystallization during post-cold- rolling annealing

Fig. 5 presents the EBSD images of the cold rolled samples in one-step and two-step homogenized conditions. It can be seen that a banded grain structure along rolling direction was developed during cold rolling and fine substructure was formed within the elongated bands in both homogenized samples. The subgrain size varied considerably from grain to grain and within each grain. Although the microstructure and recrystallization fraction before cold rolling were largely different between one-step and two-step homogenized samples (Fig. 4c vs. 4d), there was almost no difference in microstructure after cold rolling between two homogenized samples. The average subgrain size becomes almost the same, which are determined to be 0.66 μm and 0.67 μm for one-step and two-step homogenized samples, respectively. It was reported that the misorientation of low angle grain boundaries increased with strain and could eventually become high angle grain boundaries [25, 26]. It is observed that, besides the original high angle grain boundaries, some additional high angle grain boundaries were also formed during cold rolling in both homogenized samples. In addition, EBSD analysis results show that the grain boundaries after cold rolling are predominant by low angle grain boundaries for both homogenization conditions. Almost 65% of the boundaries were low angle boundaries in both cases, and the average misorientation angles were determined to be 13.2º and 12.8º for one-step and two-step homogenized samples, respectively.

Figs. 6 and 7 show the evolution of microstructure after isochronal annealing (for 1 h) at the temperature range of 200 - 500 ºC for one-step and two-step homogenized samples, respectively. It is found that both homogenization condition and annealing temperature have significant effect on the recrystallization microstructure. At the low annealing temperatures up to 250 ºC (Fig. 6a and Fig. 7a), both one-step and two-step homogenized samples were mainly recovered structure. Due to very low recrystallized fraction and small recrystallized grains, no obvious microstructure change was observed with compared to the cold rolled samples (Fig. 5). As the annealing temperature reaches to 300 ºC (Fig. 6b and Fig. 7b), typical partially recrystallized microstructures that composed of recrystallized, recovered grains and elongated deformed regions were present in both homogenized samples. Compared to the one-step homogenized sample in which the large and elongated

recrystallized grains consumed a large part of the surrounding deformed matrix with a preferentially growth along the rolling direction, static recrystallization in the two-step homogenized sample produced a large number of very fine grains within deformed bands and there was very limited elongated grains growing along rolling direction. The large and elongated recrystallized grains only occurred at 400 ºC for the two-step homogenized sample. When the annealing temperature ≥ 400 ºC, the difference in microstructure between one-step and two-step homogenized samples becomes more significant (Fig. 6c and Fig. 7c). The original deformed structure in the one-step homogenized sample was completely consumed by the recrystallized and recovered grains at the temperature of 400 ºC, while a considerable amount of deformed structure remained in the matrix of the two-step homogenized sample. Further increase of the annealing temperature from 400 to 500 ºC leads to slightly grain coarsening and these grains become more equiaxed in the one-step homogenized sample (Figs. 6d and 6e). However, the structure of two-step homogenized sample consisted of duplex partially recrystallized structure in which coarse elongated grains, small equiaxed grains and some deformed regions co-existed (Figs. 7d and 7e). Even after annealing at 500 ºC for 1 h, a small amount of deformed regions with low angle grain boundaries still remained in the matrix. In addition, it is worth noticing that while the one-step homogenized samples had less pronounced elongated grain structure, the recrystallized and recovered grains are highly elongated in the two-step homogenized sample. This is probably due to the fact that the high number density of Al_3Zr dispersoids obtained by two-step homogenization can exert much higher Zener drag force on grain boundary migration during recovery and recrystallization processes. Compared with that of one-step homogenized samples, the recrystallization process is obviously postponed to higher annealing temperature for the two-step homogenized sample.

Fig. 8 displays the recrystallized fraction and grain size a function of annealing temperature. With increasing annealing temperature, both the fraction and grain size of recrystallized grains increased in both homogenized samples. At low annealing temperatures (≤ 300 ºC), a relative low recrystallization rate and recrystallized grain coarsening are observed. At 300 ºC, the recrystallized fraction is only 11% and 7% and the average recrystallized grain size is 2.2 μm and 1.7μm for one-step and two-step homogenized samples, respectively. When annealed beyond 300 ºC, fast increases of recrystallized fraction with increasing temperature in both homogenized samples are observed (Fig. 8a). The recrystallized grain size increases very slowly at the temperature ranges of 200 to 300 ºC and 200 to 350 ºC for one-step and two-step homogenized samples, respectively. Beyond these

temperatures, the average grain sizes increase rapidly with increasing annealing temperature (Fig. 8b). Compared with one-step homogenized samples, the two-step homogenized samples generally have lower recrystallized fraction and smaller recrystallized grain size under all annealing conditions. Furthermore, a significant difference of recrystallized fractions between both homogenized samples are at the temperature range of 400-450 ºC, whereas the difference of recrystallized grain sizes between both homogenized samples becomes more significant at the annealing temperature range of 350-450 ºC. The recrystallization temperature was defined as the temperature at which 50% recrystallization has been completed [7]. It can be seen from Fig. 8(a) that, the recrystallization temperatures are around 400 and 470 ºC for one-step and two-step homogenized samples, respectively. Compared with one-step homogenization, the two-step homogenization increases the recrystllization temperature by 70 ºC.

Fig. 9 shows the average misorientation and subgrain size as a function of annealing temperature for both homogenized samples. For one-step homogenized samples, there is a continuous increase in average misorientation with increasing annealing temperature until the hardness value reaches a plateau at the temperatures of 400-450 ºC. Conversely, there is only a small change in the average misorientation at low annealing temperatures (≤300 ºC) for two-step homogenized samples. Beyond 300 ºC, the average misorientation increase continuously but moderately with increasing annealing temperature. Because of low recovery and recrystallization rate, two-step homogenized samples generally have a significant lower average misorientation at all annealing temperatures (Fig. 9a). On the other hand, when annealed below 300 ºC, very fine subgrain sizes similar to that of cold rolled condition are obtained in both homogenized samples (Fig. 9b). At high annealing temperatures (beyond 300 ºC), the subgrain growth rate becomes high and their size increases continuously with increasing annealing temperature. Compared to one-step homogenized samples, two-step homogenized samples have smaller subgrain size, especially at the temperature range of 300-500 ºC The above quantitative measurement results indicate that the two-step homogenization has a strong effect on hindering subgrain growth, which can be explained by a high number density of Al_3Zr dispersoids that exert a strong pinning effect on dislocation and sub-grain boundary motions.

The variation of Vickers microhardness as a function of temperature for both one-step and two-step homogenized samples after isochronal annealing are given in Fig. 10. It is noted that the one-step and two-step homogenized samples exhibit a similar variation trend. Three regions were exhibited: (1) decrease in microhardness (≤300 ºC); (2) increase in hardness

(300 ºC to 470 ºC); (3) decrease in microhardness (≥470 ºC). As confirmed by microstructure observations and recrystallized fraction measurement (Fig. 6 to Fig. 8), the onset of recrystallization in the two-step homogenized samples is postponed to higher temperature compared to that of one-step homogenized samples. Moreover, the backscattered electron images in Fig. 11 shown the intermetallic particles in the cold-rolled sample and the evolution of intermetallic particles during isochronal annealing in both one-step and two-step homogenized samples (the evolution of intermetallic particles in both conditions nearly the same). It is reveals that, there are mainly two types of coarse intermetallic particles exist in the matrix for cold-rolled sample. In addition, a large number of fine intermetallic particles are observed. Based on previous studies [27, 28], SEM-EDS results suggest that the coarse intermetallic particles exhibited bright and grey contrast in the backscattered electron SEM images are determined to be η($MgZn_2$) and S(Al_2CuMg), respectively. And the fine intermetallic particles are also determined to be η($MgZn_2$). These η($MgZn_2$) particles are probably formed during cooling after hot rolling and subsequent annealing. With the temperature increase, there is only significant small area fraction of intermetallic particles dissolved into the matrix when annealed ≤ 300 ºC (Fig. 11a and Fig. 11b). Hence, the first region of decrease in Vickers microhardness for both one-step and two-step homogenized samples is related to the process of recovery and recrystallization. After that, as the annealing temperature increased beyond 300 ºC (Fig. 11c to Fig. 11e), intermetallic particles are gradually dissolved into the matrix with the temperature increase. And most of the intermetallic particles are dissolved into the matrix when annealing temperature reach to 470 ºC, beyond which the area fraction of intermetallic particles remain nearly constant. Combined with microstructure observation, it can be concluded that the region of Vickers microhardness increase for both one-step and two step homogenization conditions was attributed to solution hardening surpass the recovery and recrystallization softening, the increase of recrystallized fraction and the growth of the recrystallized grains result in the second region of Vickers microhardness decrease. In addition, after detailed investigation, the Vickers microhardness of two-step homogenized samples decrease less dramatically than that of one-step homogenized samples in the temperature range of ≤ 300 ºC. This is apparently due to the more significant recovery and recrystallization degree in one-step homogenized samples.

3.4 Discussion

The EBSD results (Fig. 6-9) clearly indicated that different homogenization treatments strongly affected the recrystallization process of 7150 alloy containing 0.13% Zr during post-cold-rolling annealing. In general, recrystallization process involves the formation of strain-free subgrains and the subsequent growth at the expense of surrounding deformed matrix. A critical radius R_C for the subgrains be able to grow into the surrounding matrix is given by the Gibbs-Thomson relationship [7, 29]:

$$R_C = \frac{4\gamma_{GB}}{P_D - P_Z} \qquad (1)$$

where γ_{GB} = 0.32 J/m^2 is the specific grain boundary energy, P_D is the driving force due to the stored deformation energy and P_Z is the retarding force (Zener drag) from dispersoids exert upon the dislocation and subgrain boundaries.

It can be seen from this equation that, at a critical value of P_Z, the Zener drag will become sufficient to overcome the driving force and recrystallization will be stalled.

The expression of driving force P_D for recrystallization is given as follow [29]:

$$P_D = \frac{Gb}{\delta_{SB}}\left[\frac{\alpha\theta}{4\pi(1-\nu)}\ln\left(\frac{e\theta_C}{\theta}\right) + 0.5C_P^2\frac{b}{\delta_{SB}}\right] \qquad (2)$$

Where G ~2.65 × 10^{10} N/m^2 is the shear modulus, b = 2.86 × 10^{-10} m is the burgers vector, δ_{SB} is the average subgrain size after deformation, α is the geometric constant expect to have a value of 3, θ is the average subgrain misorientation, ν ~ 0.33 is the poisson ratio, θ_C (of the order of 15°) is the critical misorientation for a high angle boundary, C_P is an alloy-dependent constant (of the order of 5).

A widely used relationship for the Zener drag P_Z of coherent dispersoids is given by **[7]**:

$$P_Z = \frac{3\gamma_{GB} f_V}{2r} \qquad (3)$$

where f_V and r are the local volume fraction and the radius of the dispersoids, respectively. It is obviously that small dispersoids with a high volume fraction (*i.e.*, a high f/r value) is necessary in order to achieve a high Zener drag P_Z to overcome the driving force for grain boundary migration and achieve high recrystallization resistance.

Table 3 shows the average misorientation θ, subgrain size δ_{SB} and the driving force P_D measured or calculated from EBSD maps after cold rolling for one-step and two-step homogenized samples. From Eq. (1), we can find that subgrains with higher driving force P_D are favor of nucleation and growth for recrystallized grains. Whereas, the values of driving force P_D for one-step and two-step homogenized samples are 1140.5 KJ·m^{-3} and 1103.7

$KJ \cdot m^{-3}$ respectively, and the difference of driving force P_D between these two samples is insignificant. As for the fact that one-step and two-step homogenized samples have nearly the same driving force P_D, the change of the recrystallization behavior result from driving force for both one-step and two-step homogenized samples during isochronal annealing is negligible.

To find out the underlying reason for the differences in recrystallization behavior between one-step and two-step homogenized samples, the precipitation behavior of Al_3Zr dispersoids during different homogenization conditions should be considered. Table 2 shows the volume fraction f_V, the radius r and number density N_V of the Al_3Zr dispersoids after one-step and two-step homogenization. Those Al_3Zr dispersoids which precipitated during homogenization have excellent thermal stability during hot rolling and subsequent heat treatment, and strong retarding effect on subgrain and grain boundaries is obtained during isochronal annealing. According to Eq. (3), the Zener drag P_Z becomes larger as the f/r ratio increase, and the calculated Zener drag p_z of the Al_3Zr dispersoids for one-step and two-step homogenized samples are shown in Table 2. It is shown that the Zener drag P_Z in the two-step homogenized sample is 160.5 $KJ \cdot m^{-3}$, which is more than 2 times of that in the one-step homogenized sample with Zener drag P_Z of 73.8 $KJ \cdot m^{-3}$. Hence, for the two-step homogenized sample which own smaller size with higher number density of Al_3Zr dispersoids, the remarkable higher recrystallization resistance is obtained. According to Eq. (1), critical subgrain size for subgrains to grow into the surrounding deformed matrix in two-step homogenized samples is larger than that of in the one-step homogenized samples. Therefore, the subgrains in the two-step homogenized samples have greater difficulties to become recrystallized grains due to the Zener drag from Al_3Zr dispersoids. In the two-step homogenized sample, even after annealed at 500 ^oC, the retained fine subgrains revealed that the Al_3Zr dispersoids provide sufficient Zener drag to prevent subgrains to become recrystallized grains, and this will lead to a great decrease in recrystallized fraction. In comparison, the one-step homogenized sample which own lower Zener drag, under certain annealing temperature, fine subgrain is hardly to see.

The precipitation of Al_3Zr dispersoids during homogenization also affect the growth velocity of subgrain and grain boundaries, thus further affect the fraction and size of recrystallized grains. The increase in recrystallized fraction and recrystallized grain size with increasing annealing temperature can be explained by the increased mobility of grain boundaries at higher temperature. However, for two-step homogenized samples, the

migration of subgrain and grain boundaries were strongly retarded during annealing, and this will yielded lower recrystallization kinetics. In contrary, the one-step homogenized sample have a less retarding effect on the migration of subgrain and grain boundaries, and this will led to higher recrystallization kinetics. As plotted in Fig. 8 and Fig. 9, recrystallized fraction, recrystallized grain size and cell size increase with the increase of annealing temperature. However, the subgrains in the two-step homogenized samples are less prone to growth out from the deformed matrix and the growth rate of recrystallized grains is low because of the higher Zener drag P_Z from Al_3Zr particles. Consequently, the process of recrystallization then requires more time or higher temperatures to complete in two-step homogenized samples. Furthermore, the recrystallized grain size, recrystallized fraction and cell size in two-step homogenized sample is smaller than that of one-step homogenized sample at each annealing temperature. In addition, when annealed at temperature ≤ 300 ºC, mainly recovery occurs in the form of nucleation and growth of subgrains within the deformed matrix. In turn, as shown in Fig. 9, it lead to only a slightly increase of average misorientation angle and cell size. Annealed above 300 ºC, the subgrains are able to grown into the deformed matrix, and the recrystallized microstructure increase significantly with annealing temperature increase. The recrystallization result in a significant increase of high angle boundaries and cell size.

5. Conclusions

The effect of two-step homogenization on the recrystallization behavior of 7150 Al alloy during during isochronal annealing after cold-rolling in the temperature range of 200 ºC to 500 ºC has been studied. The softening behavior has been monitored by microhardness measurement, and the microstructure in terms of grain structure was characterized by EBSD method. Measured recrystallized fraction, recrystallized grain size, average misorientation and cell size were also used to characterize the microstructure change. Furthermore, the precipitation behavior of Al_3Zr dispersoids and the activation energy for the normal grain growth were discussed. Compared with that of one-step homogenized sample, the following conclusions can be made based on the results presents in current study.

(1) The two-step homogenization used for 7150 Al alloy strongly promotes the rystallization resistance during hot rolling. A significant recrystallization occurred in the one-step homogenized samples which have a recrystallized fraction more than 61% with an average recrystallized grain size of ~ 21 μm. With respect to the two-step homogenized samples, the majority of the microstructure was typically recovered structure having a recrystallized fraction ~ 8% with an average recrystallized grain size of ~ 10 μm. However,

the subgrain size becomes almost the same after cold rolling, which are 0.66 μm and 0.67 μm for one-step and two-step homogenized samples, respectively. In addition, grain boundaries in both cases are predominantly low angle grain boundaries, and almost 65% of the boundaries have low angle grain boundaries.

(2) The difference in microstructure between these two homogenized samples is hardly to see when annealed below 250 ºC. When annealing at 300 ºC, both one-step and two-step homogenized samples have a microstructure containing elongated coarse grains and equiaxed small grains. However, there are only very few large grains present in two-step homogenized sample compared to that of one-step homogenized sample. After the annealing temperature ≥ 350 ºC, compared with the microstructure of one-step homogenized samples consisted of partial recrystallized microstructure with dominant of elongated coarse grains, the structure of two-step homogenized samples consisted of partial recrystallized structure containing elongated caorse grains and equiaxed small grains. The original deformed structure in one-step homogenized sample was completely consumed by the recrystallized and recovered grains at the temperature beyond 400 ºC. However, the original deformed structure is gradually consumed by the growing of recrystallized and recovered grains in the two-step homogenized samples, and there were still some deformed regions remained even after annealing at 500 ºC.

(3) Two-step homogenization appears to be more effective in suppressing recrystallization. Compared with that of one-step homogenized samples, two-step homogenized samples own a generally lower recrystallized fraction and smaller recrystallized grain size under all annealing conditions. And two-step homogenization increases the recrystllization temperature by 120 ºC compared with that of one-step homogenized sample. In addition, a significant lower average misorientation and smaller cell size were obtained in two-step homogenized samples compared with that of one-step homogenized samples after annealing. The variation of Vickers microhardness in both cases is very similar, and the increase in microhardness is due to the dissolve of secondary particles.

(4) Compared with one-step homogenized sample, two-step homogenization result in significant smaller size of Al_3Zr particles with considerable much higher density. With respect to insignificant difference in volume fraction, the average sizes of Al_3Zr particle are determined to be ~18.9 nm and ~ 7.8 nm for one-step and two-step homogeninzed samples, respectively.

Acknowledgments

The authors would like to acknowledge the financial support from the Natural Sciences and Engineering Research Council of Canada (NSERC) and from Rio Tinto Alcan through the NSERC Industrial Research Chair in Metallurgy of Aluminum Transformation at the University of Québec at Chicoutimi. The authors would also like to thank Dr. Z. Zhang for his help in TEM observation.

References

[1] J.P. Immarigeon, R.T. Holt, A.K. Koul. Light weight materials for aircraft applications. Mater Charact 1995; 35:41-67.

[2] A. Heinz, A. Haszler, C. Keidel. Recent development in aluminium alloys for aerospace applications. Mat Sci Eng A 2000; 280:102-107.

[3] J.C. Williams, E.A. Starke. Progress in structural materials for aerospace systems. Acta Mater 2003; 51:5775-5799.

[4] E.A. Starke, J.T. Staley. Application of modern aluminum alloys to aircraft. Prog Aerosp Sci 1996; 32:131-172.

[5] P. Mukhopadhyay, M. Loeck, G. Gottstein. A cellular operator model for the simulation of static recrystallization. Acta Mater 2007; 55:551-564.

[6] E. Nes, N. Ryum, O. Hunderi. On the Zener drag. Acta Metall 1985; 33:11-22.

[7] F.J. Humphreys, M. Hatherly. Recrystallization and Related Annealing Phenomena, 2rd ed.. Elsevier science Inc., Oxford, 2004.

[8] J.D. Robson, P.B. Prangnell. Predicting recrystallised volume fraction in aluminium alloy 7050 hot rolled plate. Mater Sci Tech 2002; 18:607-614.

[9] J.D. Robson, P.B. Prangnell. Modelling Al_3Zr dispersoid precipitation in multicomponent aluminium alloys. Mater Sci Eng A 2003; 352:240-250.

[10] B. Morere, R. Shahani, C. Maurice, J. Driver. The influence of Al3Zr dispersoids on the recrystallization of hot-deformed AA 7010 alloys. Metall Mater Trans A 2001; 32:625-632.

[11] A.R. Eivani, H. Ahmed, J. Zhou, J. Duszczyk. An experimental and theoretical investigation of the formation of Zr-containing dispersoids in Al-4.5Zn-1Mg aluminum alloy. Mater Sci Eng A 2010; 527:2418-2430.

[12] E. Clouet, J.M. Sanchez, C. Sigli. First-principles study of the solubility of Zr in Al. Phys Rev B 2002; 65:094105.

[13] K.E. Knipling, D.C. Dunand, D.N. Seidman. Nucleation and precipitation strengthening in dilute Al-Ti and Al-Zr alloys. Mat Sci Eng A 2007; 38A:2552-2563.

[14] K.E. Knipling, D.C. Dunand, D.N. Seidman. Precipitation evolution in Al-Zr and Al-Zr-Ti alloys during isothermal aging at 375-425 ºC. Acta Mater 2008; 56:114-127.

[15] K.E. Knipling, D.N. Seidman, D.C. Dunand. Ambient- and high-temperature mechanical properties of isochronally aged Al-0.06Sc, Al-0.06Zr and Al-0.06Sc-0.06Zr (at.%) alloys. Acta Mater 2011; 59:943-954.

[16] J.D. Robson. Optimizing the homogenization of zirconium containing commercial aluminium alloys using a novel process model. Mat Sci Eng A 2002; 338:219-229.

[17] Z.H. Jia, G.Q. Hu, B. Forbord. Enhancement of recrystallization resistance of Al-Zr-Mn by two-step precipitation annealing. Mat Sci Eng A 2008; 483-484:195-198.

[18] X.Y. Lu, E.J. Guo, P. Rometsch, L.J. Wang. Effect of one-step and two-step homogenization treatments on distribution of Al_3Zr dispersoids in commercial AA7150 aluminium alloy. T Nonferr Metal Soc 2012; 22:2645-2651.

[19] Y.L. Deng, Y.Y. Zhang, L. Wan, A.A. Zhu, X.M. Zhang. Three-Stage Homogenization of Al-Zn-Mg-Cu Alloys Containing Trace Zr. Metall Mater Trans A 2013; 44:2470-2477.

[20] B.L. Ou, J.G. Yang, M.Y. Wei. Effect of Homogenization and Aging Treatment on Mechanical Properties and Stress-Corrosion Cracking of 7050 Alloys. Metall Mater Trans A 2007; 38A:1760-1773.

[21] Z.Y. Guo, G. Zhao, X.-G. Chen. Effects of two-step homogenization on precipitation behavior of Al_3Zr dispersoids and recrystallization resistance in 7150 aluminum alloy. Mater Charact 2015; 102:122-130.

[22] F.J. Humphreys. Review grain and subgrain characterisation by electron backscatter diffraction. J Mater Sci 2001;36:3833-3854.

[23] C. Mondal, A.K. Mukhopadhyay. On the nature of T($Al_2Mg_3Zn_3$) and S(Al_2CuMg) phases present in as-cast and annealed 7055 aluminum alloy. Mat Sci Eng A 2005; 391:367-376.

[24] Y. Deng, Z.M. Yin, F.G. Cong. Intermetallic phase evolution of 7050 aluminum alloy during homogenization. Intermetallics 2012; 26:114-121.

[25] H. Jazaeri, F.J. Humphreys. The transition from discontinuous to continuous recrystallization in some aluminium alloys: I -the deformed state. Acta Mater 2004; 52:2329-3250.

[26] W.C. Liu, J.G. Morris. Effect of pre-treatment on recrystallization and recrystallization textures of cold rolled CC AA 5182 aluminum alloy. Mat Sci Eng A 2003; 363:253-262.

[27] D.K. Xu,P.A. Rometsch,N. Birbilis. Improved solution treatment for an as-rolled Al-Zn-Mg-Cu alloy. Part I. Characterisation of constituent particles and overheating. Mat Sci Eng A 2012; 534:234-243.

[28] D.K. Xu,P.A. Rometsch,N. Birbilis. Improved solution treatment for an as-rolled Al-Zn-Mg-Cu alloy. Part II. Microstructure and mechanical properties. Mat Sci Eng A 2012; 534:244-252.

[29] H.E. Vatne, T. Furu, R. Ørsund, E. Nes. Modelling recrystallization after hot deformation of aluminium. Acta Mater 1996; 44:4463-4473.

Table 1

Chemical composition of the 7150 alloy studied (in wt%).

Zn	Mg	Cu	Zr	Fe	Si	Ti	Al
5.51	1.88	2.29	0.13	0.06	0.03	0.01	Bal.

Table 2

Dispersoid radius r, numer density N_V and volume fraction f_V of Al_3Zr dispersoids as well as the calculated P_Z in one-step and two-step homogenized samples.

Alloy	Homogenization	r (nm)	N_V (μm^{-3})	f_V (%)	P_Z ($KJ \cdot m^{-3}$)
7150 with 0.13%Zr	One-step	18.9	104	0.29	73.8
	Two-step	7.8	1260	0.26	160.5

Figures

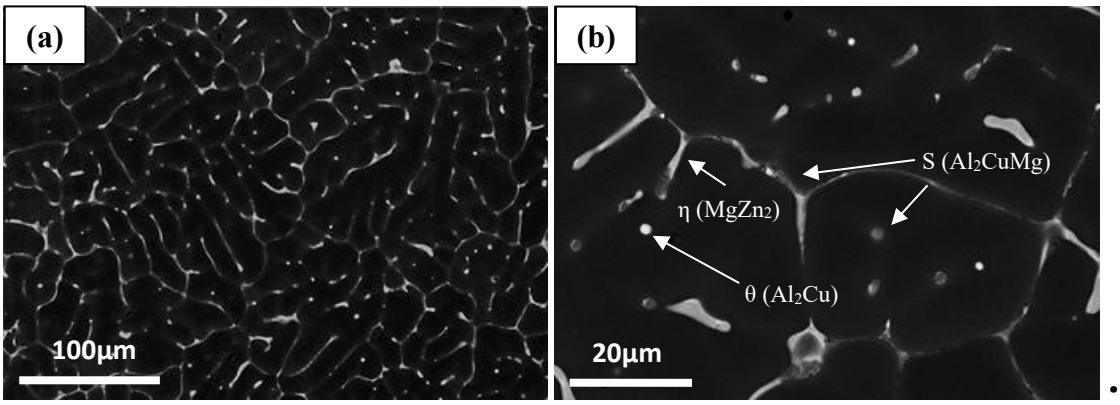

Fig. 1. Backscattered SEM images of the as-cast 7150 alloy microstructure:

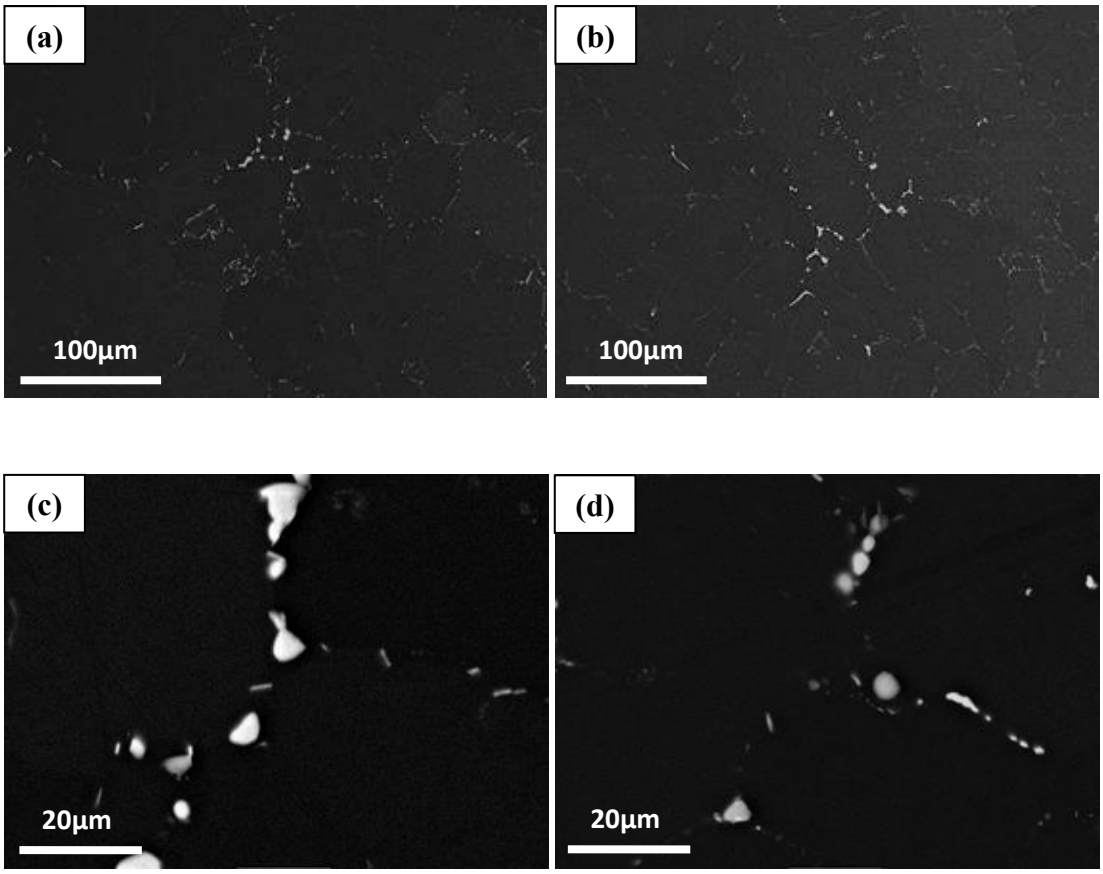

Fig. 2. Backscattered SEM images of the homogenized microstructure of 7150 alloy:

(a) low and (c) high magnification for one-step homogenization;

(b) low and (d) high magnification for two-step homogenization.

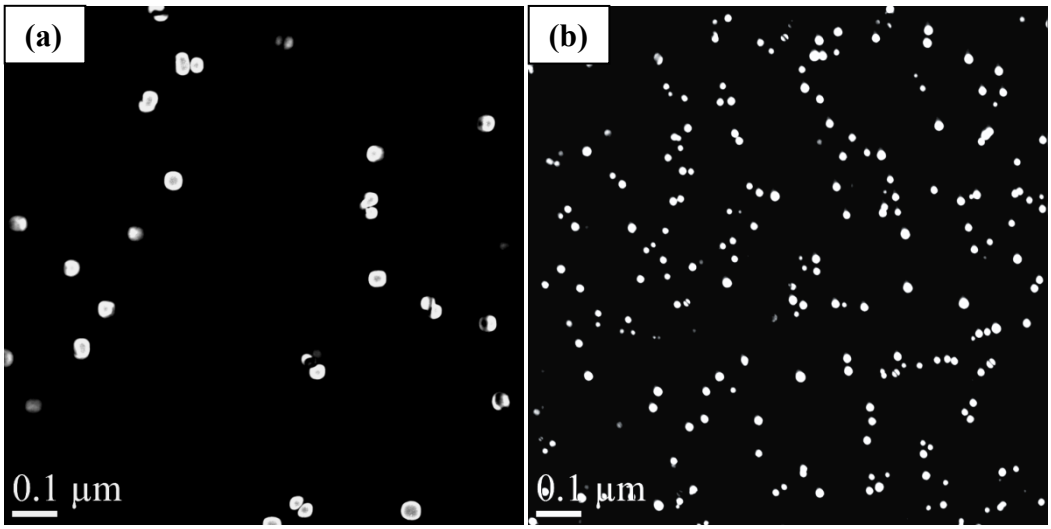

Fig. 3. Typical TEM centered dark field images of the size and distribution of Al_3Zr dispersoids after one-step and two-step homogenization treatments:

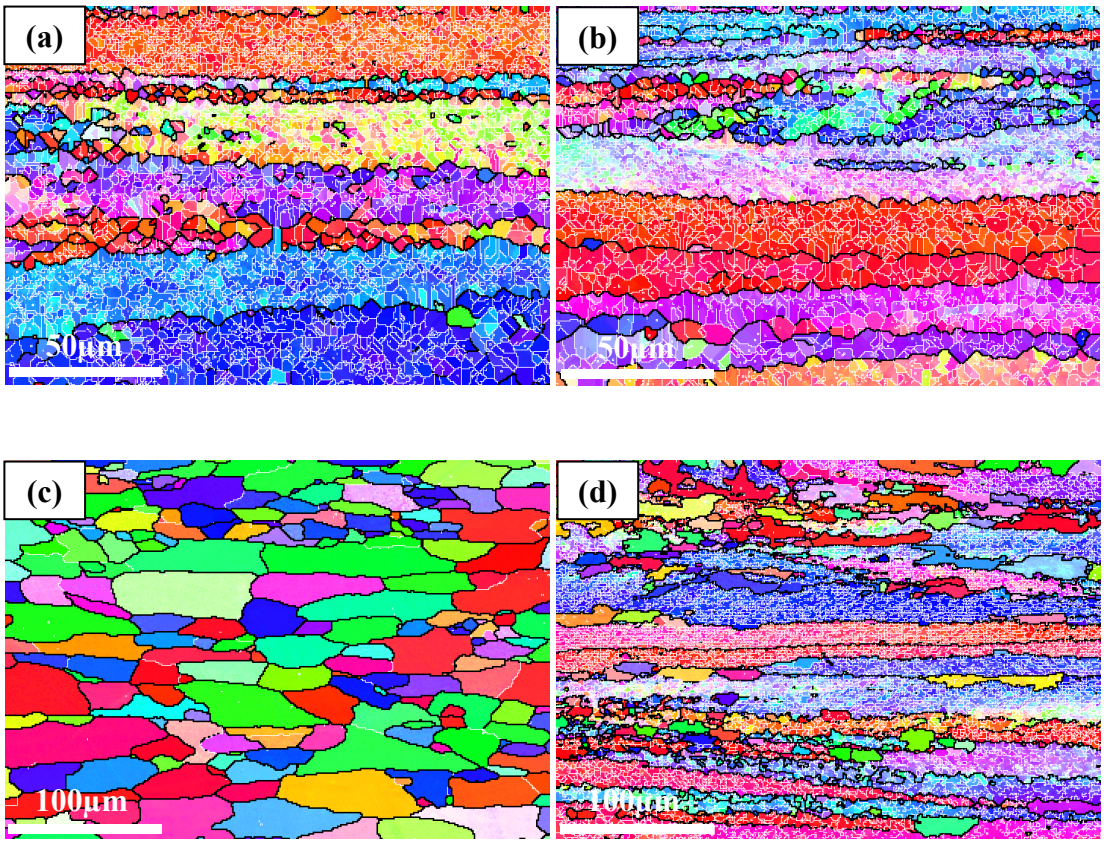

Fig. 4. EBSD images of the samples after hot rolling and subsequent annealing:

(a) one-step homogenization and hot rolled, (b) two-step homogenization and hot rolled, (c) one-step homogenization, hot rolled and annealed at 400 °C/2 h, (d) two-step homogenization, hot rolled and annealed at 400 °C/2 h.

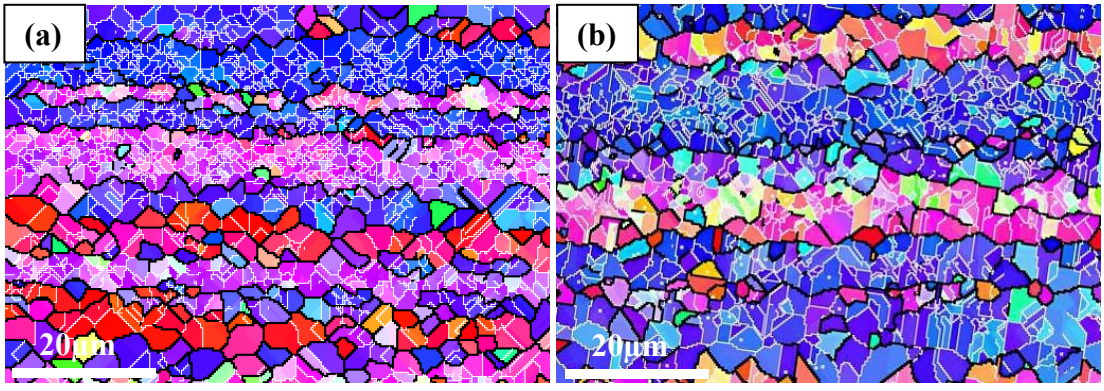

Fig. 5. EBSD images of the samples after cold rolling:

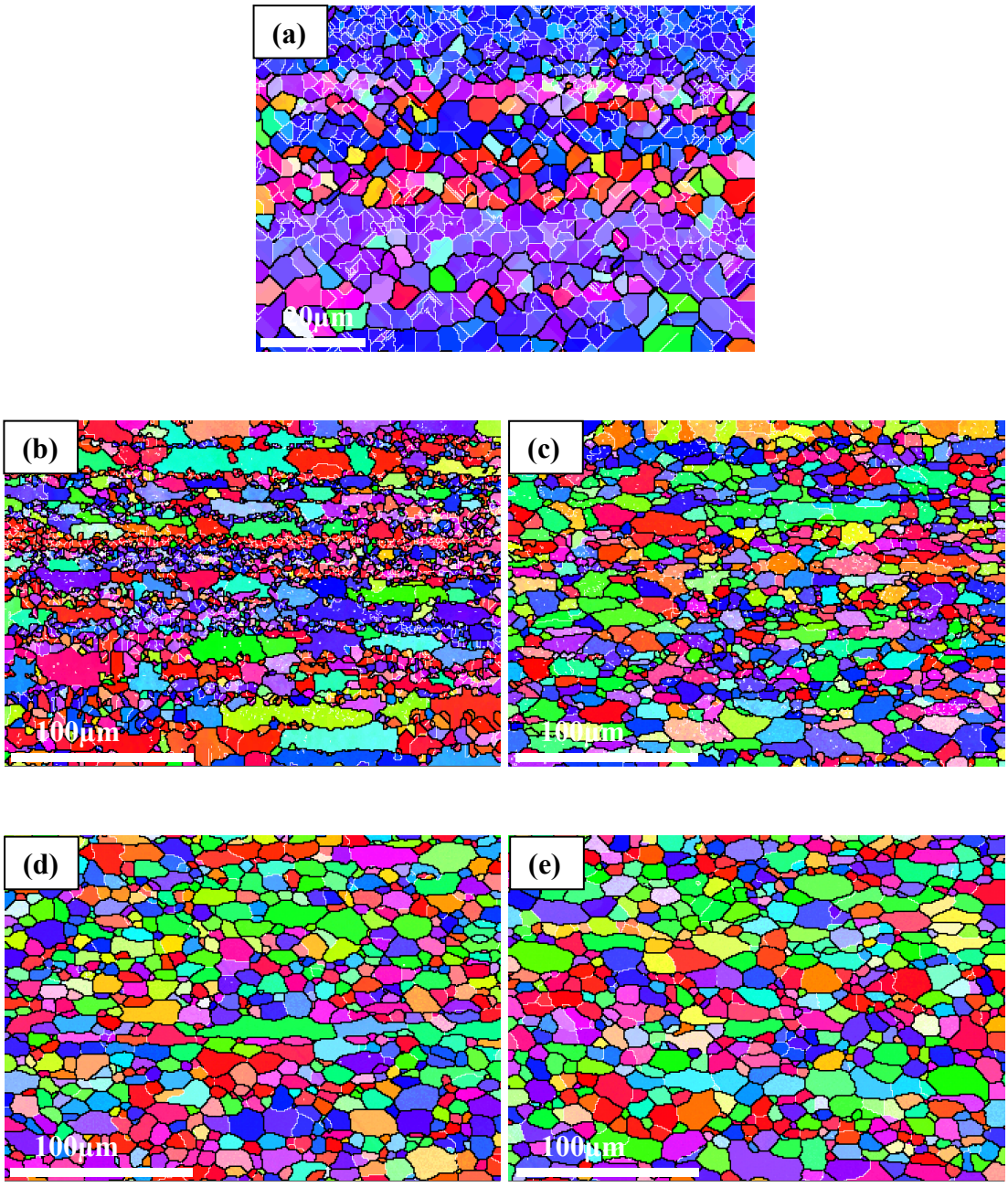

Fig. 6. Typical EBSD images of one-step homogenized and cold rolled samples after isochronal annealing for 1 h at different temperatures: (a)250 ºC, (b)300 ºC, (c) 400 ºC, (d)470 ºC, (e) 500 ºC.

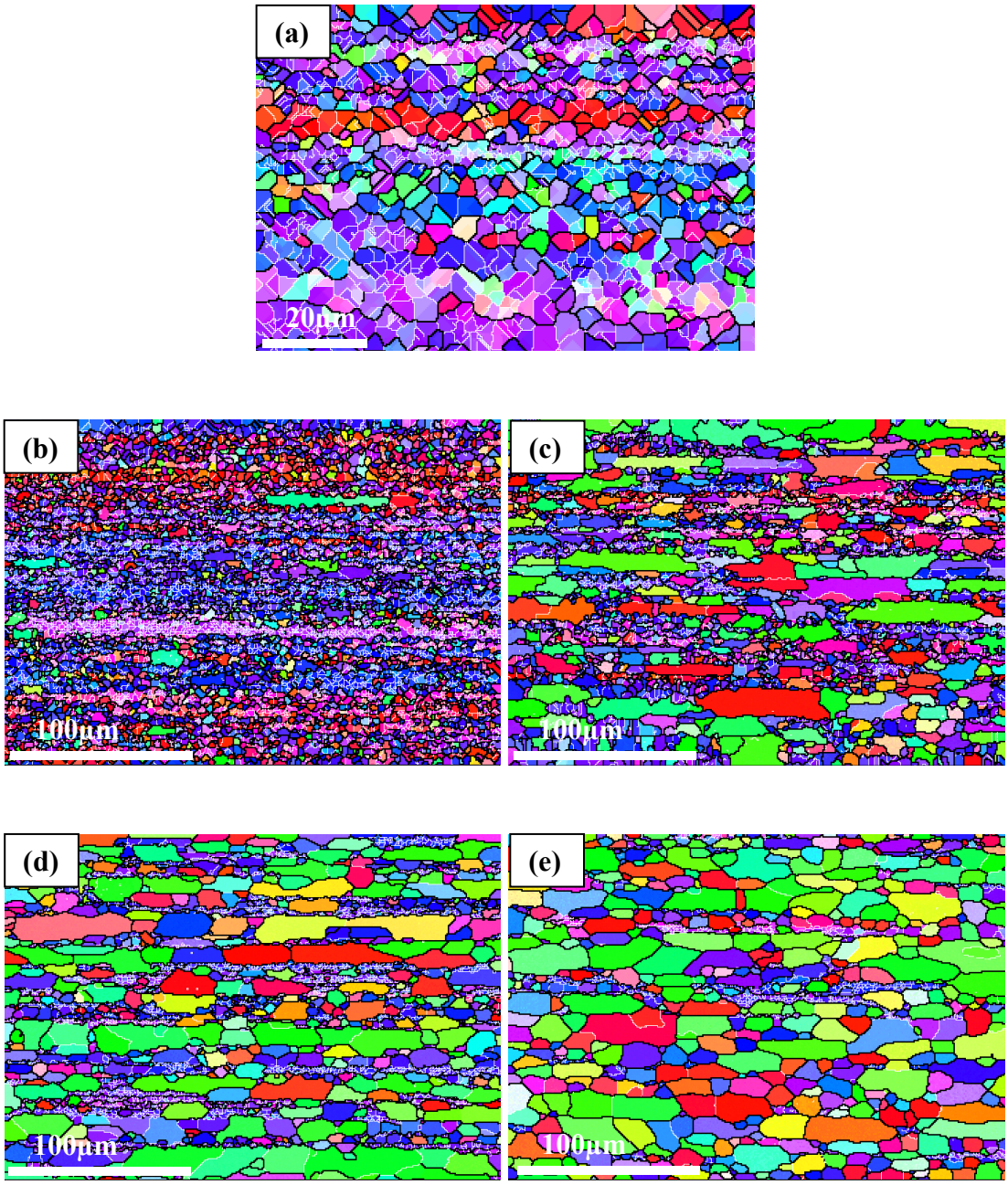

Fig. 7. Typical EBSD images of two-step homogenized and cold rolled samples after isochronal annealing for 1 h at different temperatures: (a)250 ºC, (b)300 ºC, (c) 400 ºC, (d)470 ºC, (e) 500 ºC.

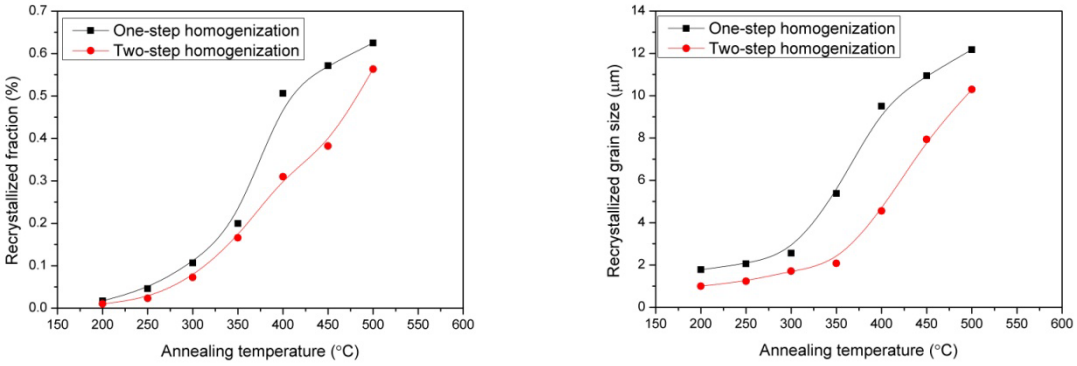

Fig. 8. Recrystallized fraction (a) and grain size (b) as a function of temperature annealing.

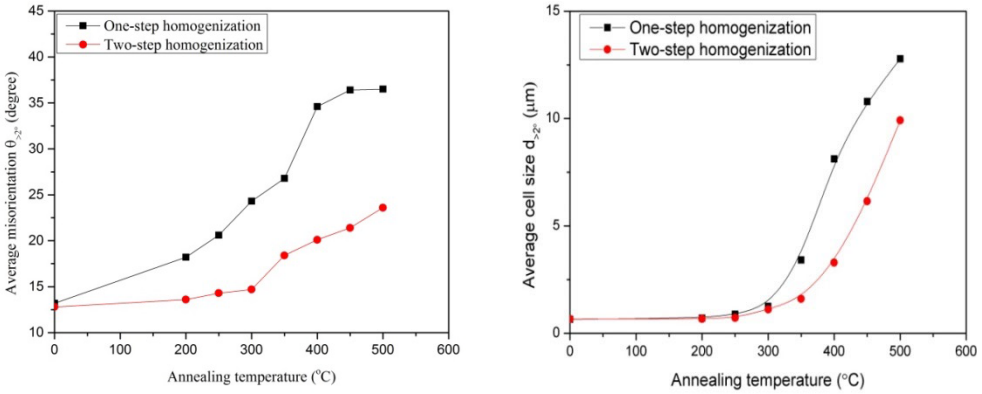

Fig. 9. Evolution of average misorientation (a) and subgrain size (b) as a function of annealing temperature

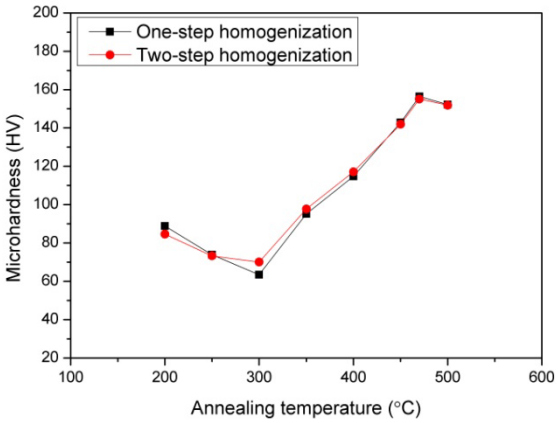

Fig. 10. Evolution of the Vickers microhardness as a function of annealing temperature.

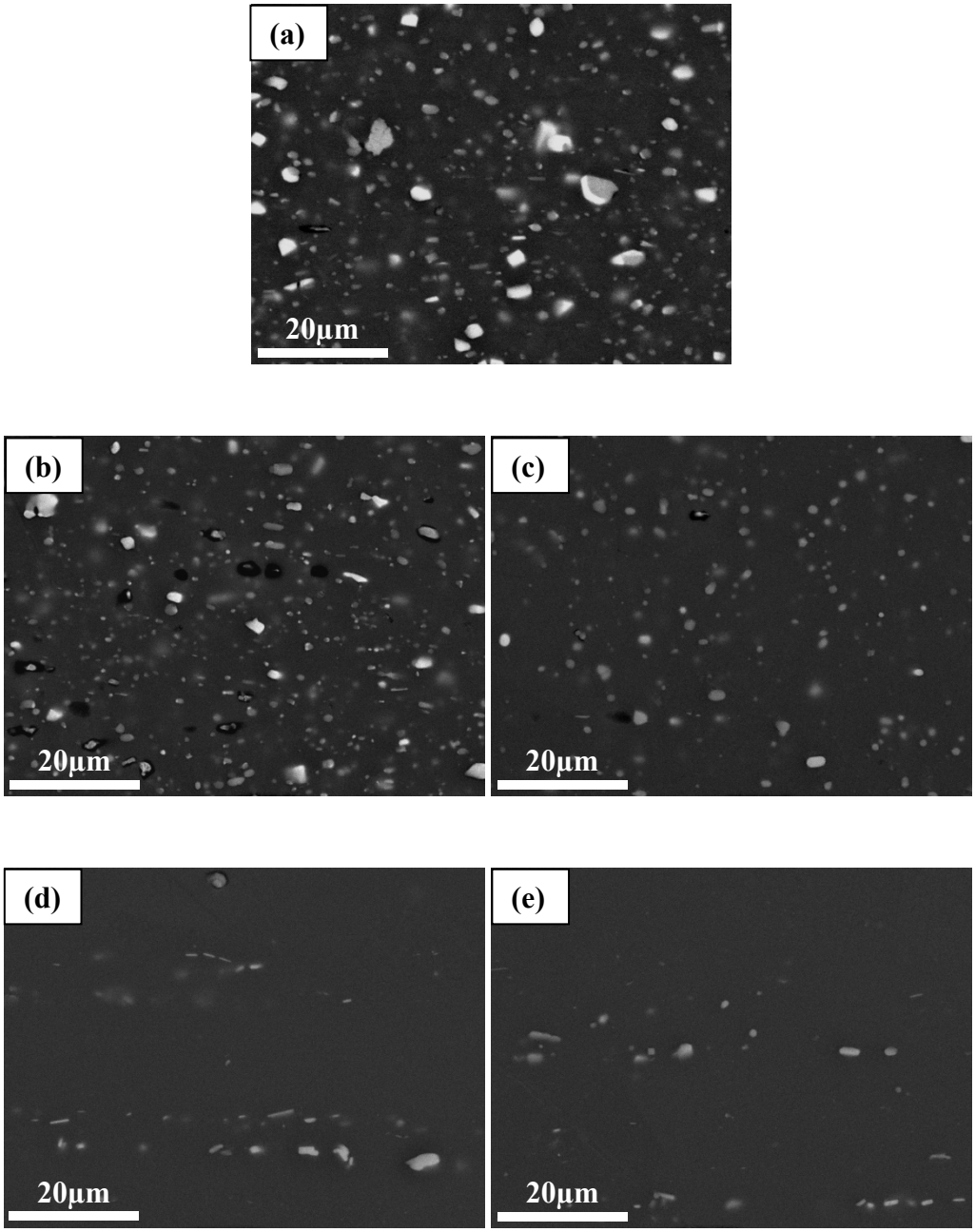

Fig. 11. Evolution of the second phases with change of annealing temperature: (a)250 ºC, (b)300 ºC, (c)400 ºC, (d)470 ºC, (e)500 ºC.